Vietnam Journal of Catalysis and Adsorption
Tạp chí xúc tác và hấp phụ Việt Nam

https://chemeng.hust.edu.vn/jca/

Investigation of $CuMnO_x$ spinel catalyst for toluene oxidation

Tran Thi Thu Hien [2,3], Ly Bich Thuy[2], Pham Thi Mai Phuong[4], Le Minh Thang[1*]

[1]*School of Chemical Engineering, Ha Noi University of Science and Technology, 01 Dai Co Viet, Ha Noi, Viet Nam*
[2]*School of Environmental Science and Technology, Ha Noi University of Science and Technology, 01 Dai Co Viet, Ha Noi, Viet Nam*
[3]*Faculty of Natural Sciences , Quy Nhon University, 170 An Duong Vuong, Quy Nhon City, Binh Dinh, Viet Nam*
[4]*Advanced Institute for Science and Technology, Hanoi University of Science and Technology, 1 Dai Co Viet, Hanoi, Vietnam*
**Email: thang.leminh@hust.edu.vn*

ARTICLE INFO

Received: 31/8/2021
Accepted: 17/9/2021
Published: 24/9/2021

Keywords:

$CuMnO_x$ spinel catalyst, toluene, solgel method

ABSTRACT

$CuMnO_x$ spinel catalyst, prepared by the sol-gel method, and characterized by modern techniques such as XRD, BET, H_2-TPR, EPR, were used to oxide toluene in the temperature range from 150°C to 400°C . Among, the investigated catalysts as MnO_2, CuO, and $CuMnO_x$, the $CuMnO_x$ showed the highest catalytic activity. It converted 100% toluene to CO_2 at 250°C in excessed oxygen conditions. The higher catalytic performance of $CuMnO_x$ than MnO_2, CuO because of its higher specific surface area and its lower reduction temperature. The results also implied that the interaction between Cu and Mn could improve the reduction capacity of $CuMnO_x$ catalyst. In summary, the $CuMnO_x$ catalyst is a promising catalyst for toluene treatment.

Introduction

Volatile organic compounds (VOCs) are polluted substances of great concern because of their impact on the environment and human health [1]. Among VOCs treatment methods, oxidation is a useful method to treat VOCs. Howver, the technique requires high temperature to remove VOCs effectively. Catalytic oxidation is considered as one of the most effective methods to treat VOCs due to the high destruction efficiency at low temperature [2].

The proficiency of catalysts depended on nature and the preparation method. The noble metal-based catalyst are popularly used for VOC oxidation due to high catalytic activity at low temperatures. Besides those, transition metal-based catalyst are also commercially available and comparatively cheaper than precious metal catalysts [3]. Nowadays, the transition metal oxides such as manganese oxides, cobalt oxides, nickel oxides, copper oxides, and mixed metal oxide catalysts were widely investigated. They exhibited high catalytic activity for the oxidation of toluene [4-11]. Among those, copper and manganese are cheaper and more plentiful than nickel and cobalt [12].

In previous studies, the spinel catalyst are one of the most popular mixed transition metal oxides catalysts because of their effective economy [13]. The metal in spinel structure is mostly transitions metal oxides as Mn, Cu, etc. The spinel's general formula is AB_2O_4. The catalysts with the spinel structure have cubic and A cations located in tetrahedral sites, B cations in octahedral sites [14]. Therefore, spinel oxides are applied for numerous technology. The preparation

https://doi.org/10.51316/jca.2021.068

methods of spinel catalyst consist of sol-gel [14], hydrothermal, co-precipitation [15] and so on.

In recent studies, the $CuMnO_x$ co-precipitation catalyst is one of the well–known transition metal oxides catalysts for CO oxidation at ambient temperature with cheap cost, high catalytic activity. Besides, many literature works show that the catalyst has also been focused on the VOCs oxidation reaction such as propene, toluene, etc [16,17,18]. It has active oxygen species related to Cu and can oxidize CO entirely at room temperature [3]. The performances of $CuMnO_x$ catalysts also were significantly influenced by their structure and preparation method. The presence of manganese oxide can promote CuO reduction, and plays a particular role in oxygen donors [14]. Moreover, it has been studied that the $CuMnO_x$ catalysts have no activity after calcinating at temperatures over 500°C, where spinel structure has been formed [3]. Many studies also revealed that spinel transition metal oxides of copper, manganese with general formula AB_2O_4 had long – time stability [12].

Thus, the above information demonstrated that the $CuMnO_x$ catalyst has the potential for VOCs oxidation as toluene. Besides, the Mn–Cu spinel oxide sol-gel catalysts have not been studied for the oxidation of toluene. The research has been investigated to synthesize the Mn–Cu mixed oxides catalyst by sol-gel method and determine its catalytic activity for toluene oxidation process.

Experimental

Preparation of the catalysts

$CuMnO_x$ catalyst was prepared by sol gel method. A solution of $Mn(NO_3)_2$ 50% 0.33 M was mixed to solution Cu $(NO_3)_2.3H_2O$ 0.17 M with molar ratio of Mn/Cu was 1.94 then they formed a solution. Afterward, 20% citric acid solution 0.95 M was added to the solution. The solution was heated to 60°C and evaporated at this temperature until a sticky gel was obtained. The product was dried at 120°C for 12h and calcined at 500°C in air for 3h at a heating rate of 1 min/°C. The catalyst was assigned as $CuMnO_x$.
Copper oxide and manganese oxide catalysts were prepared under the same conditions and assigned as CuO and MnO_2.

Catalyst characterization

The specific surface areas of the catalysts were determined by N_2 adsorption using a Micromeritics Gemini VII 2390 instrument, GeViCat center, Hanoi University of Science and Technology.

The X-ray diffraction (XRD) patterns were obtained on a D8 Advance Bruker instrument, Faculty of Chemistry, Hanoi University of Science, Vietnam.

The Autochem II 2920 device at GeViCat center, Hanoi University of Science and Technology was used to record H_2 -TPR profile.

EPR spectra were characterized using EMX, micro X system (Brucker, Germany), GeViCat center, Hanoi University of Science and Technology.

The catalyst was also characterized by Nicolet IS50 FT – IR spectrometer, GeViCat center, Hanoi University of Science and Technology.

Catalytic oxidation experiment

The powdered catalyst (0,1 g) was placed in a micro stainless steel reactor. An N_2 flow went through the toluene tank to bring toluene vapor to the microreactor. The inlet toluene flow (about 5000 ppm) was kept stable, and the outlet flow was detected by an online gas chromatograph (GC) with a thermal conductivity detector (TCD). The oxidation reaction was conducted in a micro reactor.

Analysis and calculation of the results

Toluene conversion was determined by the folllowing equation:

$$\eta_{T\ (\%)} = \frac{C_T^o - C_T^i}{C_T^i} X\ 100 \quad (1)$$

Where, $\boldsymbol{\eta_T}$**:** toluene conversion (%);
$\boldsymbol{C_T^i}$**:** toluene concentration of inlet flow at a temperature T (ppm) ;
$\boldsymbol{C_T^o}$**:** toluene concentration of outlet flow at a temperature T (ppm).
The conversion of toluene to CO_2 was calculated as equation 2:

$$\gamma_{CO_2\ (\%)} = \frac{C^0_{CO_2,T}}{7\left(C_T^o - C_T^i\right)} X\ 100 \quad (2)$$

Where, $\boldsymbol{\lambda_{CO_2}}$**:** the conversion of toluene to CO_2 (%); $\boldsymbol{C^i_{CO_2,T}}$**:** CO_2 concentration of inlet flow at a temperature T (ppm);

https://doi.org/10.51316/jca.2021.068

$C^{0}_{CO_2,T}$: CO_2 concentration of outlet flow at a temperature T (ppm).

The g-value or g-tensor for EPR spectra [19] was determined in equation 3:

$$h.\nu_O = \Delta E = g\beta H_o$$

Where, h: Planck's constant =6.62 10^{-34} J.s

ν_O: The magnetic field of frequency (Hz)

g: g value (g tensor)

H_o: Magnetic field (induction) in Tesla

β: Bohr magneton = 9,2740154 10^{-24} J/T

Results and discussion

Characterization of the catalyst

BET surface

BET surface areas of synthesized catalysts are presented in Table 1.

Table 1: BET surface areas of the catalysts

No	Catalysts	BET surface area (m^2/g)
1	$CuMnO_x$	25.15
2	CuO	1.50
3	MnO_2	14.44

The BET surface of the $CuMnO_x$, CuO, and MnO_2 catalyst were 25.15; 1.50 and 14.44 m^2/g respectively. The results showed that $CuMnO_x$ catalyst has the largest BET surface area. The CuO and MnO_2 catalyst possessed lower surface area, especially CuO catalyst has very small BET surface area of 1.5 m^2/g. The fact that the combination formation between Cu and Mn positively affects the catalyst's surface area.

XRD

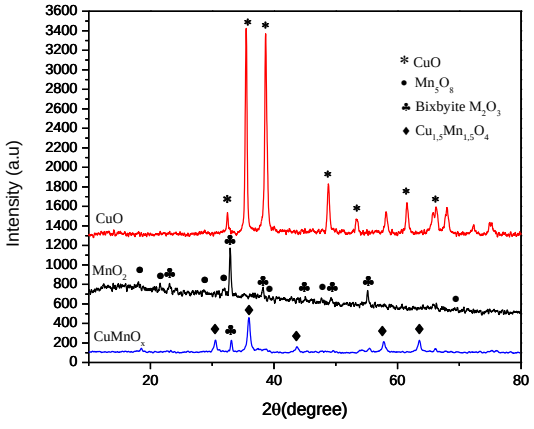

Figure 1: XRD pattern of samples

The $CuMnO_x$ catalyst was characterized by the XRD technique to determine the phase identification and crystalline sizes. The XRD analysis of the catalyst showed the diffraction peaks at 2θ: 30.53°; 35.93°; 43.66°; 57.74°; 63.45° respectively which corresponds to the lattice (220), (311), (400), (333), (440) of the spinel crystal structure $Cu_{1.5}Mn_{1.5}O_4$ [20]. The pattern clearly shows the formation of $Cu_{1.5}Mn_{1.5}O_4$ in the sample. Besides, an amount of Mn_2O_3 was detected in the sample. Thus, the $CuMnO_x$ catalyst has been synthesized successfully.

On the characteristic diffraction XRD of the two pure oxide catalysts, it it is observed the structure of CuO at values 2θ of 32.48°; 35.52°; 38.64°; 48.8°; 53.3°; 61.7 ° ; 66.2° correspond to the (110), (002), (111), (202), (020), (113) and (311) [21]. Besides, The XRD pattern of MnO_2 indicated the diffraction peaks at 2θ: 32.9° (222); 38.28° (400); 45.06° (332); 49.16° (134); 55.16° (440) of bixbyite Mn_2O_3 and structure of Mn_5O_8 was seen in the catalyst [22-24].

The crystalline sizes of samples were determined by the Scherer equation [25], as show in Table 2.

Table 2: Crystalline size of the catalysts

No	Samples	Crystalline sizes (nm)
1	$CuMnO_x$	14.45
2	CuO	22.94
3	MnO_2	23.64

As a result, it was recorded that pure oxide catalysts prepared by the sol-gel method produced larger particle sizes than mixed oxides catalysts; and the formation of mixed oxide between Cu and Mn led to the decrease of crystalline sizes.

H2 – TPR

Figure 2 displays H_2 – TPR pattern of $CuMnO_x$, MnO_2 and CuO catalysts.

To explain clearly the reason for the higher catalytic activity of the $CuMnO_x$ solgel, TPR- H_2 measurements were shown to determine the oxidation-reduction properties of the catalysts, as Fig. 2.

https://doi.org/10.51316/jca.2021.068

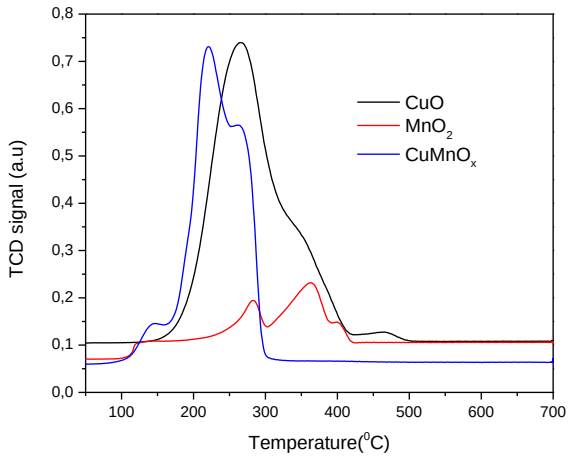

Figure 2: H2 – TPR pattern of samples

Table. 3: Consumed hydrogen amount (mol/g) of two pure single oxides (MnO_2, CuO) and the mixed oxides ($CuMnO_x$)

Catalysts	Consumed hydrogen (mmol/g)	Temperature at maximum (°C)
MnO_2	0.63035	282.4
	2.12913	364.1
CuO	10.2312	26.,2
	0.0666	466.9
$CuMnO_x$	0.0235	141.6
	0.3215	235.3
	0.2031	275.1

The TPR profile for MnO_2 displayed two peaks, centred at 282.4 and 364.1°C, assigned to the reduction of MnO_2 to Mn_xO_y [26, 27].

The TPR profile for CuO consisted of two peaks, assigned to the reduction of CuO, *i.e.*, Cu^{2+} to Cu^{+} (265.2°C) and $Cu^{+}$to CuO (466.9 °C) [28- 29].

In spinel $CuMnO_x$ catalyst, a significant change in the TPR profile was observed. The reduction of MnO_2 was shifted to lower temperatures. Three main reduction peaks corresponding to the reduction of MnO_2 to Mn_2O_3 (141°C), Mn_2O_3 to Mn_3O_4 (235.3°C), and Mn_3O_4 to MnO (275.1 °C) could be observed [30].

The total mol of consumed hydrogen in spinel catalyst also decreased. These effects may be due to the interactions of Mn-Cu oxides. Results obtained from H_2-TPR showed that the interactions Mn-Cu oxides in the spinel catalyst can reduce the reduction temperature of the catalyst. It means that the spinel catalyst can catalyze the oxidation reaction at the lower temperature than pure MnO_2 or CuO catalyst.

EPR spectra of samples

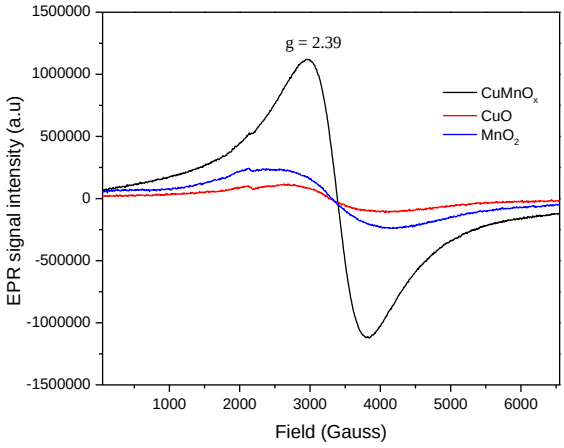

Figure 3: EPR profile of catalysts

The EPR spectra of all studied samples are shown in Figure 3. EPR spectroscopy was employed to obtain additional information on the nature of the active phase species. The spectrum of the $CuMnO_x$ catalyst displays an axial symmetry with a calculated g = 2.39. This signal was assigned to isolated Cu^{2+} ions in octahedral coordination with tetragonal distortion. The lack of EPR signal characteristic for Mn species revealed that most likely they exist as Mn^{4+}[31,32].

IR spectra of samples

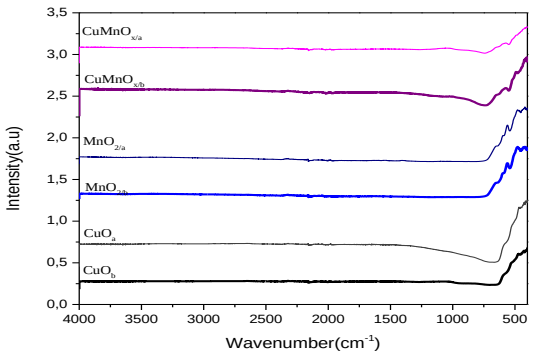

Figure 4 : IR profile of catalysts

https://doi.org/10.51316/jca.2021.068

Figure 4 shows IR spectra of pure oxides and $CuMnO_x$ catalysts. The MnO_2 catalyst before and after the reaction possessed peaks at wavenumber between 427 to 482 and 563 cm^{-1} belong to manganese oxides [33,34]. IR spectra also exhibit two vibrations appearing 476 cm^{-1}, 530 cm^{-1}, for CuO catalyst, which can be same as the vibrations of Cu-O, confirming the formation of pure CuO catalyst [35].

$CuMnO_x$ catalyst had a CuO group (530cm^{-1}), and the peaks of manganese oxides did not appear in the mixed oxides [3]. Thus, IR spectra showed no adsorbed water or organic substances on the catalyst's surface. It also means that no difference between catalysts before and after the reaction.

Catalytic activity for toluene oxidation

Toluene oxidation was performed on some catalysts labeled as $CuMnO_x$, CuO and MnO_2 The experiment results are described in Fig. 5, and Fig. 6

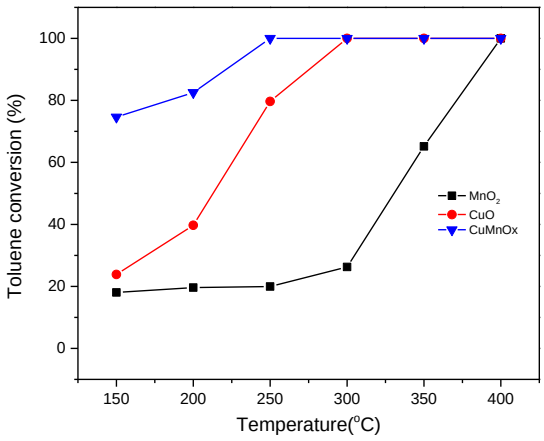

Figure 5: Toluene conversion

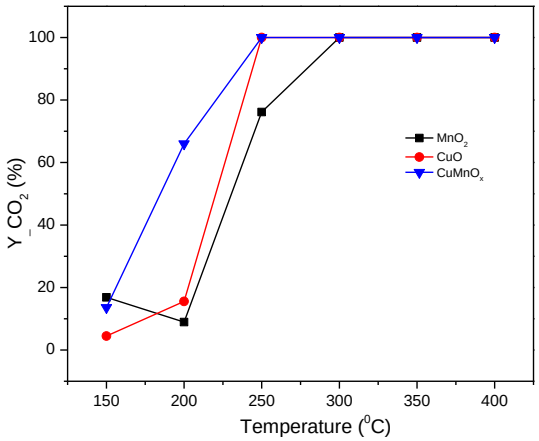

Figure 6: CO_2 yield

Results of catalyst conversion of toluene with the initial concentration of 5000 ppm are shown in Fig 5. When the reaction temperature increased from 150°C to 400°C, the toluene conversion percentage was increased. For the $CuMnO_x$ catalyst, maximum toluene conversion reached at 250°C, and the MnO_2 catalyst showed complete toluene conversion at 400°C. Meanwhile, the CuO catalyst only exhibited complete toluene conversion from 300°C. Thus, the $CuMnO_x$ catalyst indicated better catalytic performance than the pure MnO_2 and CuO catalysts (T_{100} = 250°C).

Moreover, in Fig 6, toluene is also completely converted into CO_2 at 250°C. In comparison, yield CO_2 over MnO_2 and CuO catalysts was lower at this temperature. Therefore, it could be concluded that the catalytic activity of the $CuMnO_x$ catalyst was higher than the pure CuO, MnO_2 catalyst. The reason may be that a combination between manganese and copper helps increase the ability to oxidize toluene.

In the previous studies, the $CuMnO_x$ spinel catalysts ($Cu_{1.5}Mn_{1.5}O_4$) were prepared by co-precipitation and used widely for CO oxidation (T_{100} = 120°C) [14]. However, few studies synthesized the catalysts ($Cu_{1.5}Mn_{1.5}O_4$) by the sol-gel method for toluene oxidation. Thus, our results demonstrated that the $CuMnO_x$ catalyst synthesized by sol-gel methods is a potential catalyst to apply in gaseous pollutant treatment.

Compared to the copper-doped manganese oxide nanorod catalysts (1000 ppm toluene, T_{90} = 214^{0}C) [36], $CuMnO_x$ spinel catalyst (5000 ppm toluene, T_{100} = 250^{0}C) was synthesized more simple and exhibited the high catalytic activity.

Conclusions

Copper manganese oxide catalyst, copper oxide, and manganese oxide were prepared via the sol-gel method. The combination of copper oxide and manganese oxide increase BET surface area of the copper, manganese mixed oxide catalysts, decrease the reduction temperature of the catalyst and enhance the performance of toluene oxidation.

The experimental results showed that the $CuMnO_x$ exhibited excellent catalytic performance in the toluene conversion at 250°C and completely converted toluene into CO_2 at this temperature.

Acknowledgments

https://doi.org/10.51316/jca.2021.068

Tran Thi Thu Hien was funded by Vingroup Joint Stock Company and supported by the Domestic Master/ PhD Scholarship Programme of Vingroup Innovation Foundation (VINIF), Vingroup Big Data Institute (VINBIGDATA), VINIF.2020.TS.80.
The authors thank the supports of Vingroup Joint Stock Company, VINF, VINBIGDATA.

References

1. C. H. Wang, Chemosphere 55 (2004) 11-17. https://doi.org/10.1016/j.chemosphere.2003.10.036.
2. M. Alifanti, M. Florea, V. I. Pârvulescu, Applied Catalysis B: Environmental 70 (2007) 400-405. https://doi.org/10.1016/J.APCATB.2005.10.037
3. S. Dey, N.S. Mehta, Resources, Environment and Sustainability 4 (2021). https://doi.org/10.1016/j.resenv.2021.100025
4. M. R. Morales, B. P. Barbero, Appl. Catal. B: Environmental 67 (2018) 229-236. https://doi.org/10.1016/j.apcatb.2006.05.006
5. M. Piumetti, S. Bensaid, D. Fino, N. Russo, Appl. Catal. B: Environmental 197 (2016) 35-46. https://doi.org/10.1016/j.apcatb.2016.02.023
6. Wang L., Wang Y., Zhang Y., Yu Y., He H., Qin X., Wang B., Catal. Sci. Techno 6 (2016) 4840-4848. https://doi.org/10.1039/C6CY00180G
7. G. Zhou, X. He, S. Liu, H. Xie, M. Fu, J. Indust. Eng. Chem 21 (2015) 932–941. https://doi.org/10.1016/j.jiec.2014.04.035
8. X. Xie.; Y. Li, Z. Liu, M. Haruta, W. Shen, Nature 458 (2009) 746 – 749. https://doi.org/10.1038/nature07877
9. J. C. Lou, H. W. Yang, C. H. Lin, Aerosol and Air quality Research 9 (2009) 435 – 440. https://doi.org/10.4209/aaqr.2009.05.0027
10. M. H. Habibi, B. Karimi, J. Indust. Eng. Chem, 20 (2013) 1566 – 1570. https://doi.org/10.1016/J.JIEC.2013.07.048
11. R. Manigandana, K. Giribabua, R. Suresha, L. Vijayalakshmib, A. Stephenc, V. Narayanana, Chem. Sci. Trans 2 (2013) S47 – S50. https://doi.org/ 10.7598/cst2013.10
12. A. Hadded, J. Massoudi, E. Dhahri, K. Khirouni, B.F.O.Costa, RSV Adv 10 (2020) 42542 – 42556. https://doi.org/10.1039/D0RA08405K
13. A.S. Albuquerque, M.V.C. Tolentino, J.D. Ardisson, F.C.C. Moura, R. de Mendonca, W.A.A Macedo, Cream. Int 38 (2012) 2225 – 2231. http://dx.doi.org/10.1016/jceramint.2011.10.071
14. L. N. Cai, Y. Guo, A. H. Lu, P. Branton, W. C. Li, Journal of Molecular Catalysis A: Chemical 360 (2012) 35–41. http://doi.org/10.1016/j.molcata.2012.04.003
15. S. Mobini, F. Meshkani, M. Rezaei, The 10th International Chemical Engineering Congress & Exhibition (IChEC 2018), At Isfahan Iran (2018).
16. S. Behar, P. Gonzalez, P. Agulhon, F. Quignard, D. Swierczy ´nski, Catal. Today 189 (2012) 35–41. https://doi.org/10.1016/j.cattod.2012.04.004
17. B. H. Napruszewska, A. Michalik., A. Walczyk., D. Duraczy ´nska, R. Dula, W. Rojek, L. Lity ´nska-Dobrzy ´nska, K. Bahranowski, E. M. Serwicka, Materials 11 (2018). https://doi.org/10.3390/ma11081365
18. T. J. Clarke, S. A. Kondrat., S. H. Taylor, Catal. Today 258 (2015) 610-615.
19. N. Senesi, G.S. Senesi, Encyclopedia of Soils in the Environment: Electron – spin resonance spectroscopy, Elsevier, 2005, 426 – 437. http://doi.org/10.1016/b0-12-348530-4/00209-5
20. R. B. Irawan, P. Purwanto, H. Hadiyanto, Int Conf Trop Coast Reg Eco-Dev 23 (2015) 86–92. https://doi.org/10.1016/j.proenv.2015.01.013
21. D. Zhu, L. Wang, W. Yu, H. Xie, Scientific reporters 8 (2018). https://doi.org/10.1038/s41598-018-23174-z
22. G. Zheng, W. Zhang, R. Shen, J. Ye, Z. Qin, Y. Chao, Scientific Reports 6 (2016). https://doi.org/10.1038/srep22588
23. L. Chen, T. Zhang, H. Cheng, Ryan M. Richards, Z. Qi, Nanoscale 12 (2020) 17902-179144. https://doi.org/10.1039/D0NR04738D
24. Muniz F. T. L., Miranda M. A. R., Morilla dos Santos C., Sasaki J. M., Acta Crystallographica Section A Foundations and Advances 72 (2016) 385–390. https://doi.org/10.1107/S205327331600365X
25. W. Yang, Y. Peng, Y. Wang, H. Liu, Z. Su, W. Yang, J. Chen, W. Si, J. Li, Applied Catalysis B: Environmental, 278 (2020). http://doi.org/10.1016/j.apcatb.2020.119279
26. M. H. Kim, K. H. Cho, C.H. Shin, S.E. Kang, S.W. Ham, Korean J. Chem. Eng 28 (2011) 1139-1143. http://doi.org/10.1007/s11814-011-0035-3
27. J. Xue, J. Q. Wang, G. S. Qi, J. Wang, M.Q. Shen, W. Li, J. Catal. 297 (2013) 56–64. https://doi.org/10.1016/j.jcat.2012.09.020
28. A. Bienholz, R. Blume, A. Knop-Gericke, F. Girgsdies , M. Behren, P. Claus, J. Phys.Chem. C 115 (2011) 999–1005. https://doi.org/10.1021/jp104925k

29. Z. Wang, Z. Niu, Q. Hao, L. Ban, H. Li, Y.X Zhao, Z. Jiang, Catalysts, 9 (2019). https://doi.org/10.3390/catal9010035

30. M.H. Kim, K.H. Cho, C.H. Shin, S.E. Kang, S.W. Ham, Korean J. Chem. Eng. 28 (2011) 1139-1143. http://doi.org/10.1007/s11814-011-0035-3

31. T. Tabakova, E. Kolentsova, D. Dimitrov , K. Ivanov, M. Manzoli , A. M. Venezia, Y. Karakirova, P. Petrova, D. Nihtianova , G. Avdeev, Top Catal 60 (2017) 110–122. https://doi.org/10.3390/catal8110563

32. T. H. Bennur, D. Srinivas, P. Ratnasamy, Microporous and Mesoporous Materials 48 (2011) 111–118. http://doi.org/10.1016/s1387-1811(01)00345-6

33. D. V. Azamat, A. Dejneka, J. Lancok, V. A. Trepakov, L. Jastrabik, A. G. Badalyan, Journal of Applied Physics, 111 (2011). http://doi.org/10.1063/1.4723653

34. L. Kang, M. Zhang, Z.H. Liu, K. Ooi, Spectrochimica Acta Part A 67 (2007) 864–869. https://doi.org/10.1016/j.saa.2006.09.001

35. A. Azam, A. S. Ahmed, M Oves, M.S Khan, A. Memic, International Journal of Nanomedicine 7 (2012) 3527–3535.

36. J. Hu, W. B. Li, R. F. Liu, Catalysis Today 314 (2018) 147–153. http://doi:org/10.1016/j.cattod.2018.02.009